Preprint of Models for a hydrogen supply chain in the Nordics with compressed hydrogen tube trailers and compressed hydrogen shipping

Authors:

Matthias Maier, Thomas Alan Adams II

Date Submitted: 2025-12-11

Keywords:

Abstract:

Models in Aspen Plus for loading and unloading compressed hydrogen tube trailers and compressed hydrogen ships

Record Type: Preprint

Submitted To: LAPSE (Living Archive for Process Systems Engineering)

Citation (overall record, always the latest version):	LAPSE:2025.0724
Citation (this specific file, latest version):	LAPSE:2025.0724-1
Citation (this specific file, this version):	LAPSE:2025.0724-1v1

Models for a hydrogen supply chain in the Nordics with compressed hydrogen tube trailers and compressed hydrogen shipping

Matthias Maier [a], Thomas A. Adams II [a]*

[a] Norwegian University of Science and Technology (NTNU), Department of Energy and Process Engineering, Trondheim, Norway
* Corresponding Author: thomas.a.adams@ntnu.no.

ABSTRACT

This paper developed techno-economic models for a hydrogen supply chain in the Nordic context using compressed hydrogen tube trailers for inland transport and compressed hydrogen ships for international hydrogen export. The dynamic transfer operations used in the investigated hydrogen supply chain were modelled in Aspen Plus Dynamics. Based on these models, reduced techno-economic models were developed for all supply chain elements, which were further optimized with respect to minimal supply chain costs. Results show that the total supply chain costs increase linearly with shipping distance and decrease logarithmically with hydrogen throughput.

Keywords: Hydrogen supply chain, hydrogen tube trailer, compressed hydrogen shipping, supply chain optimization, Aspen Pus Dynamics, techno-economic analysis

1. Introduction

Hydrogen has long been thought of as a renewable alternative to fossil fuels, with an expected increase in hydrogen demand in the next 30 years [1]. The European Commission announced a plan in 2022 to import 10 million tonnes of renewable hydrogen by 2030. Norway on the other hand could become a possible export nation with its large untapped renewable energy potentials [2, 3]. In 2022, Equinor and Germany's RWE proposed a plan to export hydrogen from Norway to Germany via a new hydrogen pipeline between the two countries [4]. This plan was discontinued in 2024 due to costs and insufficient demand, and Equinor stated that the hydrogen pipeline was not viable [4]. A new pipeline requires high investment costs, has low flexibility in a geographically changing market and needs thus long-term commitments from both sellers and buyers to justify the investment project. On the other hand, shipping of hydrogen such as compressed hydrogen or liquid hydrogen shipping offers more flexibility and could thus be a viable alternative. Cebolla et al. [5] found that while a hydrogen pipeline has the lowest hydrogen delivery costs for short distance transport (i.e., less than 5000 km), compressed hydrogen shipping comes in as the second cheapest option, outperforming liquid hydrogen shipping.

Many studies have been conducted on liquid hydrogen shipping [6-8], but compressed hydrogen shipping is little studied in literature. d'Amore-Domenech et al. [9] compared different options for bulk power transmission at sea, including liquid and compressed hydrogen shipping. Babarit et al. [10] investigated different options for connecting far-offshore wind converters, and considered compressed hydrogen shipping among others. Nekså et al. [11] investigated medium scale hydrogen supply chains using compressed hydrogen tube trailers and modelled the dynamic filling and emptying behavior. Reddi et al. [12] considered tube trailer transport and calculated distribution costs for different configurations.

There is no study that investigated a complete compressed hydrogen supply chain in the Nordic-European context with both compressed hydrogen tube trailer for short distance inland transport and compressed hydrogen shipping for international hydrogen export with consistent techno-economic assumptions. This study is the first to optimize the supply chain elements and operations given the bigger picture of the entire supply chain to find a minimum supply chain cost estimate.

2. Methodology

We considered a theoretical hydrogen supply chain which uses hydrogen tube trailers for inland transport and compressed hydrogen shipping for international transport as well as terminals for receiving and sending tube trailers and compressed hydrogen ships. We modelled filling and emptying operations to estimate transfer times and energy consumption as a function of equipment size. Together with cost data for investment and operation, we calculated techno-economic models for costs as a function of equipment size. Based on the

combination of these models, we optimized values for transfer times and equipment size such that the supply chain costs are minimized. This led to the creation of reduced models for costs and optimal transfer times. The reduced models include:

- Cost of hydrogen tube trailer transport as a function of transport distance
- Investment costs for optimally sized export and import cH_2 shipping terminals
- Transfer times for optimally sized export and import cH_2 shipping terminals
- Optimal cH_2 ship size as a function of hydrogen throughput and shipping distance
- Total shipping costs as a function of hydrogen throughput and shipping distance

The economic models and assumptions are valid in a Nordic context. We assumed 2024 as the base year, current technology advancements and prices and a Norwegian operating company. Moreover, our cost optimization approach follows a single-company mindset, which tries to size equipment such that the overall supply chain costs are minimal. As for shipping terminals, we only calculated investment costs, but state operating cost factors such as specific energy consumptions or estimates for maintenance and staff. In that way, the reduced models are more general, as electricity prices are location dependent.

We calculated the dynamic filling and emptying operations using Aspen Plus Dynamics with the PR-BM property package. All models assume no heat exchange with the environment, meaning that the actual end temperature might be slightly different. However, given the short transfer times and the heat transfer characteristics, we concluded that heat exchange with the environment is insignificant. A ballpark estimation showed that heat transfer with the environment leads to a 1-2°C temperature change. The estimate is based on a heat transfer coefficient of 4.5 W/m^2K (using the Nusselt relation for free convection around a horizontal cylinder [13]) to 6 W/m^2K (estimate from Zhao et al. [14]), 10°C average temperature difference between outer wall and ambient air (based on Zhao et al. [14]) and the given transfer times. For a detailed thermodynamic analysis, we direct the reader to Zhao et al. [14] and Couteau et al. [15].

As for shipping, a trip refers to the entire operation of docking and loading at the export terminal, sailing from the export terminal to the import terminal, docking and unloading at the import terminal and sailing back to the export terminal. The trip distance is thus double the one-way distance. The term shipping costs refers to the cost of a single cH_2 ship. The term total shipping costs refers to the sum of export terminal investment costs, import terminal investment costs and shipping costs. Whenever total shipping costs are calculated in this paper, they do not include operating costs for export and import shipping terminals.

3. Model elements

3.1. cH_2 Tube Trailer

3.1.1. System description

The system specification of the compressed hydrogen tube trailer is stated in Table 1. According to Reddi et al. [12], the most cost effective composite based tube trailer configuration for hydrogen transport is using pressure vessels with a 30 inch diameter and 38 foot length at 350 bar. While the analysis was conducted based on US road regulations, similar weight limits apply for semi trailers in Norway, depending on the axle configuration [16]. Thus, we assumed the same configuration. The operational window is set by the upper and lower operational pressure of the vessel. Koshelkov [17] suggested a lower pressure limit of 20-80 bar. In this study, we chose 20 bar as the lower limit, which is a common pressure limit in hydrogen pressure test standards [18]. The lower pressure limit is a trade-off between practical hydrogen load, loading and unloading time and required compressor energy for unloading. Using 20 bar as the lower limit, 7% of the theoretical storage capacity of the hydrogen tube trailer is not used. The hydrogen payload was calculated based on the upper operational hydrogen density (i.e., 350 bar, 20°C) minus the lower operational hydrogen density in the empty state (i.e., 20 bar, 20°C). For calculation of hydrogen densities at a pressure and temperature, CoolProp [19] was used, which builds on the physical property models developed by Leachman et al. [20].

3.1.2. Calculation of costs

Table 1 states the calculation for the costs of the compressed hydrogen tube trailer. We assume that the tube trailer is utilized as much as possible to achieve lowest specific transport costs due to relatively high investment costs. Assuming 7 days per year maintenance and 821 hours downtime due to breaks, the maximum utilization is 7771 h/a. This requires 4.17 employees per truck. The total number of employees for the entire fleet might be an integer number or require part-time labor. The annual capex depends on the route profile, since the annual number of trips and annual distance influence the system lifetime. The value stated is thus an example for an average one-way trip distance of 120 km. The lifetime of the truck was assumed to be 860 000 km [21], which is similar to the estimate by Tayarani et al. [22]. The cycle lifetime of the pressure vessel system was assumed to be 22 000 cycles following the ECE R134 regulation for hydrogen-fuelled vehicles. These cycle-based and kilometer-based lifetimes were then translated into years using the operation of the hydrogen tube trailer. Variable costs were assumed to be those of an average tank truck [23]. We assume a fuel consumption of 32.6 l/100km [24] during driving (loaded and empty) and no fuel consumption during terminal time. The average annual cost per truck was calculated based on the average annual

distance driven per truck, as shown in Figure 20.

3.1.3. Filling operation

During filling of a high-pressure hydrogen tank, the temperature of hydrogen and thus the tank increases. A detailed analysis of temperature change for different conditions is given by Nekså et al. [11]. Since the maximum operational temperature of the hydrogen tank is limited, it might be required to precool the hydrogen before filling. Even if temperature limit can be satisfied without precooling, it is practical to have precooling anyway, since the hydrogen density at design pressure (i.e., 350 bar) and at a temperature above 20°C is lower than the upper operational density, leading to underutilization of the pressure vessels.

The process scheme of the filling operation is depicted in Figure 4. We assumed that the tube trailer is filled from a reservoir at 350 bar which is much larger than the tube trailer, meaning that the pressure level of the reservoir is constant for the entire filling operation. First, hydrogen from the storage tank is expanded via a valve into the tube trailer until the truck reaches the same pressure level of 350 bar (upper branch in Figure 4). Before the expansion valve, hydrogen is precooled to -40°C, which we assume to be the lowest allowed precooling temperature [11]. After the expansion, the temperature in the tube trailer is 44.6°C, meaning that the upper operational density can not be reached by precooling alone. We assume that slight overfilling is allowed and use booster compressor to fill the tube trailer from 350 bar until the upper operational density is reached (lower branch in Figure 4). This happens at 369 bar at 47°C, meaning that the tube trailer pressure vessels have to be overfilled by about 20 bar.

The electric energy demand for precooling was correlated from the precooler duty using a COP of 1.1 given the correlation stated by Elgowainy et al. [25] corresponding to 20°C ambient temperature. The investment cost for the precooling unit was calculated based on the equipment cost for the precooling unit using the size correlation stated by Elgowainy et al. [25] and translated into TASC using the scheme stated in the supplementary material.

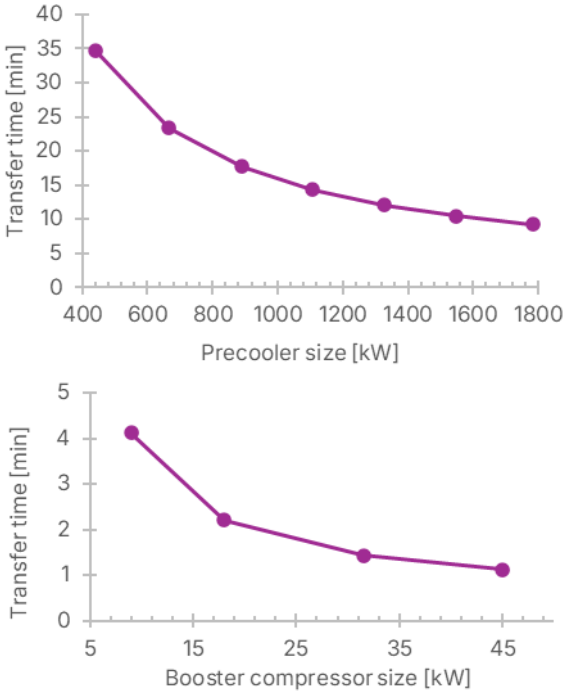

Figure 1: Trade-off for equipment sizing at filling of compressed hydrogen tube trailer (top: expansion branch, bottom: compression branch)

At the filling terminal, there is a trade-off between transfer time and equipment size (i.e., precooler and booster compressor). Larger equipment allows for higher flow rates and thus lower filling times but leads to higher cost (see Figure 1). We did not optimize this relation but chose a reasonable value instead. For the precooling unit, we chose a cooling power of 891 kW, which leads to a transfer time of 17.7 minutes for the expansion branch (see Figure 3). For the booster compressor, we chose a power of 18 kW, which leads to a transfer time of 2.2 minutes for the compression branch.

3.1.4. Storage operation

During the operation of the hydrogen tube trailer (i.e., driving from A to B), the storage tanks are subject to heat exchange with the environment. We assume that the journey time is long enough that equilibrium is reached. This means that the hydrogen pressure vessels experience isochoric cooling from the final loading temperature of 47°C to the environment temperature of 20°C, leading to a pressure decrease to 350 bar.

3.1.5. Emptying operation to a nominal pressure of 250 bar

The process scheme of the emptying operation is depicted in Figure 5. The emptying operation of the hydrogen tube trailer to a destination pressure lower than the tube trailer pressure is comprised of two parts. First, the hydrogen tube trailer can be emptied into the destination reservoir using a pressure reducing value until the pressure in the trailer drops to the storage pressure. From there on, a booster compressor is required to empty the pressure vessel further

and bring the outlet stream to the destination pressure. The booster compressor has 4 stages with intermediate cooling down to 20°C. The precooling unit in Figure 5 cools the compressed hydrogen down to 15°C to ensure a stable temperature in the storage tank. Cooling duties for intermediate cooling and precooling are not considered due to insignificance. The compressor power is controlled to achieve a desired flow rate, which was found as a trade-off between emptying time and equipment size. When the emptying branch is switched from expansion to compression, compression power gradually increases as the pressure difference between the tube trailer and the storage system increases, until the nominal power is reached (see Figure 6). The process is continued until a hydrogen density of 1.63 kg/m^3 is reached in the tube trailer, which is the equilibrium density of 20 bar and 20°C.

During emptying, the temperature in the hydrogen pressure vessels decreases due to the expansion process. The adiabatic end temperature predicted by our model is -57.8°C, which is below the safe limit of -40°C [14]. This can be avoided by increasing emptying time to allow for more heat exchange with the environment or by internal heating of the pressure vessels. The former option is not realistic due to slow heat exchange, meaning that emptying times of 3h and longer would be required. Thus, we assume that internal heating of the pressure vessels is possible. Some concepts for the implementation of heating units are described by Zhao et al. [26]. We assume that heating at the outlet based on the Joule Thomson effect is sufficient to reach a safe final temperature, but do not include an estimate for costs for the heating device. Note that the temperate drop at emptying is especially prominent in large, high-pressure vessels using composite materials. Since high tensile strengths allow for thinner walls, less vessel material is required per unit of stored hydrogen, meaning that less thermal mass is available to counteract the cooling effect at emptying.

At the emptying terminal, there is a trade-off between transfer time and equipment size (*i.e.*, booster compressor). Larger equipment allows for higher flow rates and thus lower emptying times but leads to higher cost (see Figure 2). We did not optimize this relation but chose 1350 kW as the nominal power of the booster compressor, which leads to an emptying time of 25.5 minutes.

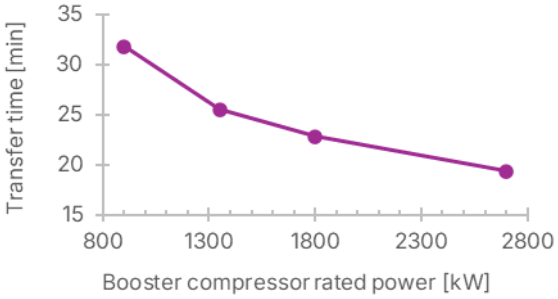

Figure 2: Trade-off for equipment sizing at emptying of compressed hydrogen tube trailer

We assume that the destination storage tank is much larger than the hydrogen tube trailer and its pressure level is thus not affected by the unloading operation. However, the pressure in the destination storage may vary in the course of one or a couple of days (e.g., hydrogen storage at a shipping terminal). While the equipment was sized for a nominal destination pressure of 250 bar, we explored the energy requirement and emptying time for different destination pressure levels (see Figure 3). Table 3 states the results of the calculations for the emptying process to 250 bar destination pressure (i.e., nominal operation). We only considered the booster compressor for costs and utility. Its TASC was calculated based on [27]. If the destination storage tank operates between pressures of 100 bar and 250 bar, the average emptying time is 20.6 minutes, and the average electricity consumption is 0.35 kWh/kgH_2.

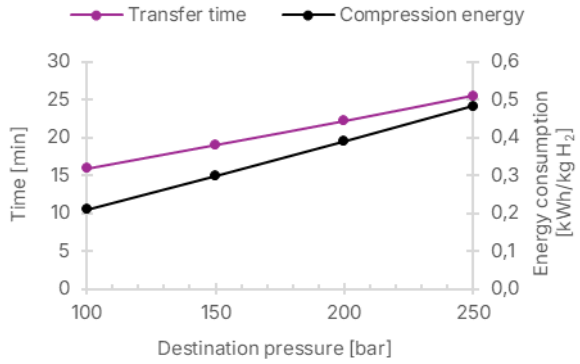

Figure 3: Emptying operation of a compressed hydrogen tube trailer – Pressure dependency

Table 1: Compressed hydrogen tube trailer specification

Parameter	Value	Unit	Source
Vessel description			
Upper pressure	350	bar	Reddi et al. [12]
Lower pressure	20	bar	Assumption
Diameter	30	inch	Reddi et al. [12]
Length	38	foot	Reddi et al. [12]
Material density	1350	kg/m^3	Reddi et al. [12]
Tensile strength	1200	MPa	Reddi et al. [12]

Wall thickness	26.1	mm	Barlow's formula with SF=2.35
Wall specific heat capacity	1246	J/kgK	Mass average based on Zhao et al. [14]
Number of vessels per truck	9	-	Reddi et al. [12]
H_2 Payload per truck			
Stored H_2 (350bar - 0bar)	893.9	kg	Calculation
Useful H_2 (350bar - 20bar)	832.1	kg	Calculation
Investment costs			
Truck	2.55	MNOK2024	Assumption
Trailer incl. pressure vessels	12.6	MNOK2024	Reddi et al. [12]
Fixed annual costs			
Annual CAPEX	3237	kNOK2024/a	Example for 120 km average distance
Truck driver costs	2965	kNOK2024/a	Supplementary material, section 1.3.2
Taxes and administration	211	kNOK2024/a	Fjeld et al. [21]
Vektårsavgift	5	kNOK2024/a	Skattetaten [28]
Variable costs	10.6	NOK2024/km	Transportøkonomisk institutt [23]

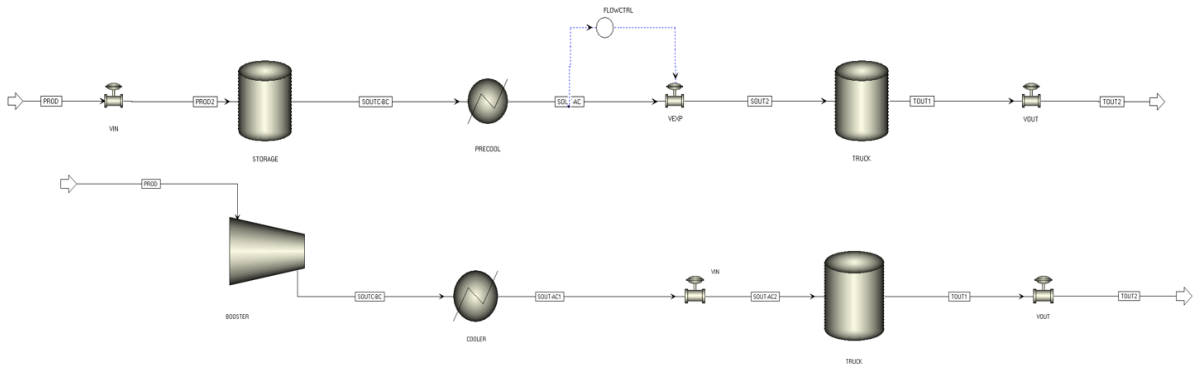

Figure 4: Filling operation of a compressed hydrogen tube trailer – Scheme

Table 2: Filling operation of a compressed hydrogen tube trailer - Specification

Parameter	Value	Unit	Source
Capital costs at filling terminal (per loading bay)			
TASC Precooling unit	30 391	kNOK2024	Correlated from [25]
TASC Booster compressor	1 113	kNOK2024	Correlated from [27]
Energy requirements			
Booster compressor – Electricity	5.9	kWh/Truck	Aspen Plus Dynamics
Precooling unit – Cooling duty	255	kWh/Truck	Aspen Plus Dynamics
Precooling unit – Electricity	232	kWh/Truck	Using COP=1.1 [25]
Precooling unit – Electricity	0.28	kWh/kg_{H2}	Calculation

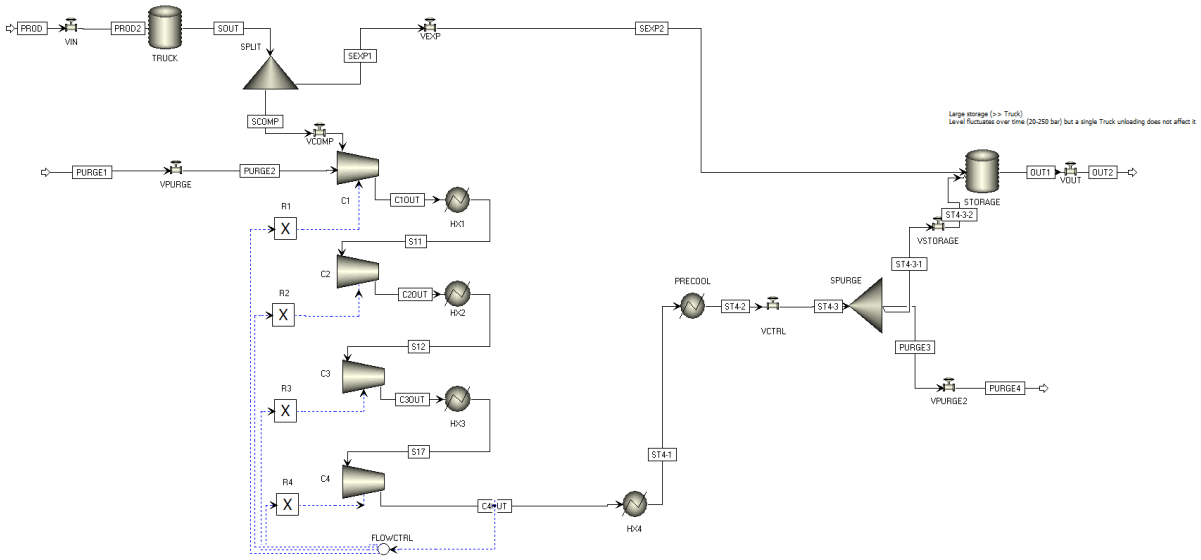

Figure 5: Emptying operation of a compressed hydrogen tube trailer – Scheme

Table 3: Emptying operation of a compressed hydrogen tube trailer – Specification

Parameter	Value	Unit
Nominal power	1350	kW
TASC	40.7	MNOK2024
Nominal electricity consumption	0.48	kWh/kg_{H2}

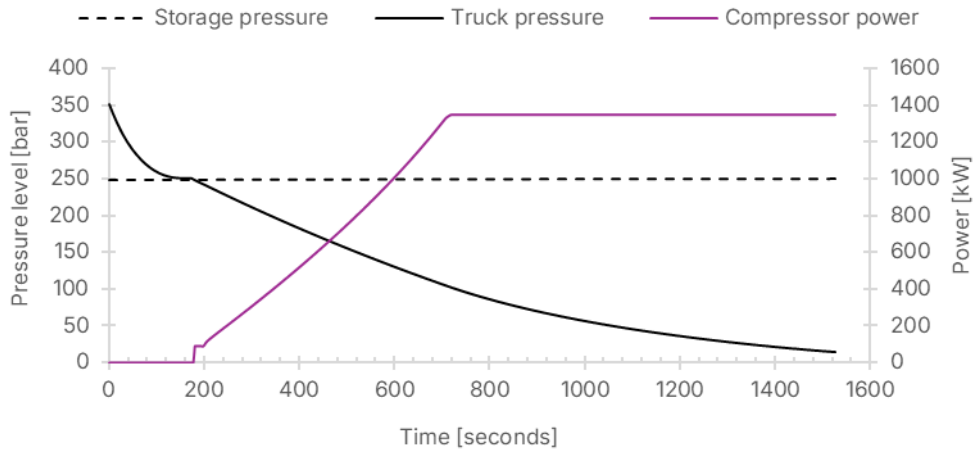

Figure 6: Emptying operation of a compressed hydrogen tube trailer to a 250 bar reservoir – Timeline

3.2. Shipping terminals for compressed hydrogen shipping (export)

3.2.1. Terminal design

Figure 8 shows the conceptual design of a shipping terminal for the export of compressed hydrogen. On the receiving side, hydrogen can be sourced from inland hydrogen production plants via cH_2 tube trailers or from on-site hydrogen production plants. For the design of the cH_2 tube trailer terminal, see section 3.1.5. At the terminal site, hydrogen is fed into an intermediate storage tank. The storage tank has a modular design and is equivalent to the hydrogen storage modules on the compressed hydrogen ships (see Table 7). The size of the storage tank was calculated as the payload of the ship minus the received hydrogen during filling of the ship. We assume a minimum storage size of 20 modules (i.e., 6178 kg cH_2) to handle short-term process interruptions and the dynamics of the ship filling operation.

On the sending side, compressed hydrogen ships can dock at the terminal and source high pressure hydrogen from this intermediate storage tank during loading. We assume a time loss of 30min for docking and undocking. The sending side has a

single-berth design, meaning that only one ship at a time can be docked and loaded. The maximum terminal throughput is thus directly linked to the size of the loading equipment. During the filling operation, the pressure level in the storage tank decreases, requiring a booster compressor and a precooling unit.

3.2.2. Model description

The process scheme of the filling operation of a cH_2 ship is depicted in Figure 9. A model in Aspen Plus Dynamics using the PR-BM property package was built to model the filling of one pressure vessel in the ship from one equally large on-land storage pressure vessel. We assume that the actual filling process consists of c filling cycles of n modules being filled simultaneously. Thus, the total filling time of a ship with n*c modules is calculated as the cycle time times the number of cycles c. The number of modules filled at the same time n is used as a linear factor to determine the size of the equipment.

The filling operation consists of two phases. First, as long as the pressure level in the terminal storage tank is larger than the pressure level in the compressed hydrogen ship, the ship is filled via the expansion branch. Herein, hydrogen flows through an expansion valve, which is opened at the start of the filling operation. The transfer time of the expansion branch is 227s.

In a second phase, a booster compressor is used to fill the ship up to the upper operational hydrogen density of 17.86 kg/m^3 (*i.e.*, density at 250 bar and 20°C). The second phase starts when the expansion valve is closed. The compression valve is opened over 100s to avoid spikes in flow rate. The booster compressor has a 4-stage design with intermediate cooling to 20°C. The power of the booster compressor is controlled to achieve a set flow rate of 50 kg/hr per vessel, which corresponds to the initial flow rate when the compression valve is opened. The controller can increase the power up to a maximum power level to achieve the flow rate set point. The model was run with different maximum set power levels, which resulted in different transfer times. The result of this analysis is stated in Figure 7, which states the total filling time of a module depending on the power of the booster compressor. Based on this relationship, we assumed that a compressor power of 640 kW per module is a reasonable trade-off and used this value for further analysis.

After compression, hydrogen is precooled to -40°C and filled to the ship. We assume no heat exchange between the precooling unit and the onboard pressure vessels. The operation stops when the upper operational hydrogen density is reached in the ship's pressure vessel. Since the temperature in the ship increases during filling, slight overfilling is required. After filling, a pressure of 273 bar and a temperature of 55°C is reached in the ship's pressure vessels. The timeline of the filling operation of one vessel / one module is stated in Figure 10.

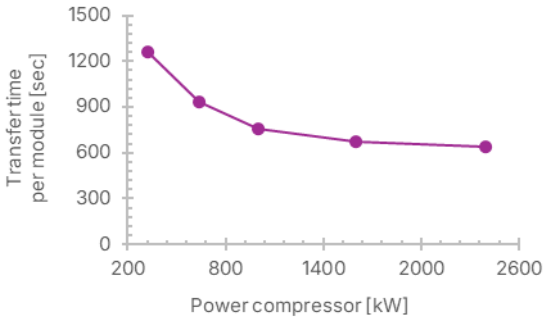

Figure 7: Trade-off for sizing of the booster compressor at compressed hydrogen export terminals

3.2.3. Investment costs

Table 4 shows the investment costs for a shipping terminal for export of compressed hydrogen. For the receiving side, we assume that the cH_2 tube trailer terminal has multiple ports where hydrogen tube trailers can dock and unload their cargo. The number of docks scales with the hydrogen throughput of the tube trailer terminal. For the design of a single dock cH_2 tube trailer terminal, see section 3.1.5. The investment costs on the sending side include the booster compressor and the hydrogen precooling unit. These are dependent on the loading rate of the cH_2 ships, which is defined by the loading time and ship size. For the terminal construction costs, we accounted for jetty and piping, which we correlated from a large scale LNG terminal [29] and scaled to the respective system size. We assume that the lifetime of the terminal is 20 years.

3.2.4. Operating costs

Table 4 states the energy requirements for the export terminal. The receiving side requires electricity for the unloading of incoming tube trailers and the sending side requires electricity and cooling water at 10°C for the loading of compressed hydrogen ships. The electricity price depends on the location within Norway. The salary cost is based on the salary for process and machine operators [30]. We assume a staff size of 4 workers. Maintenance costs were assumed to be 5% of the TPC for hydrogen conditioning.

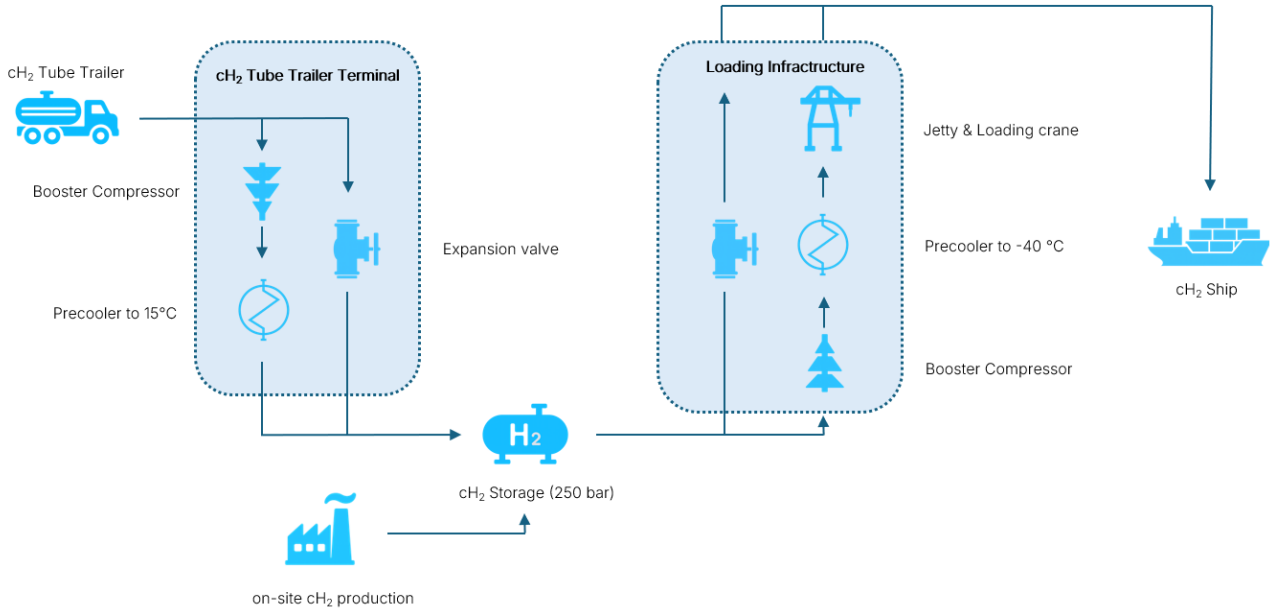

Figure 8: Process sketch of a shipping terminal for cH_2 export

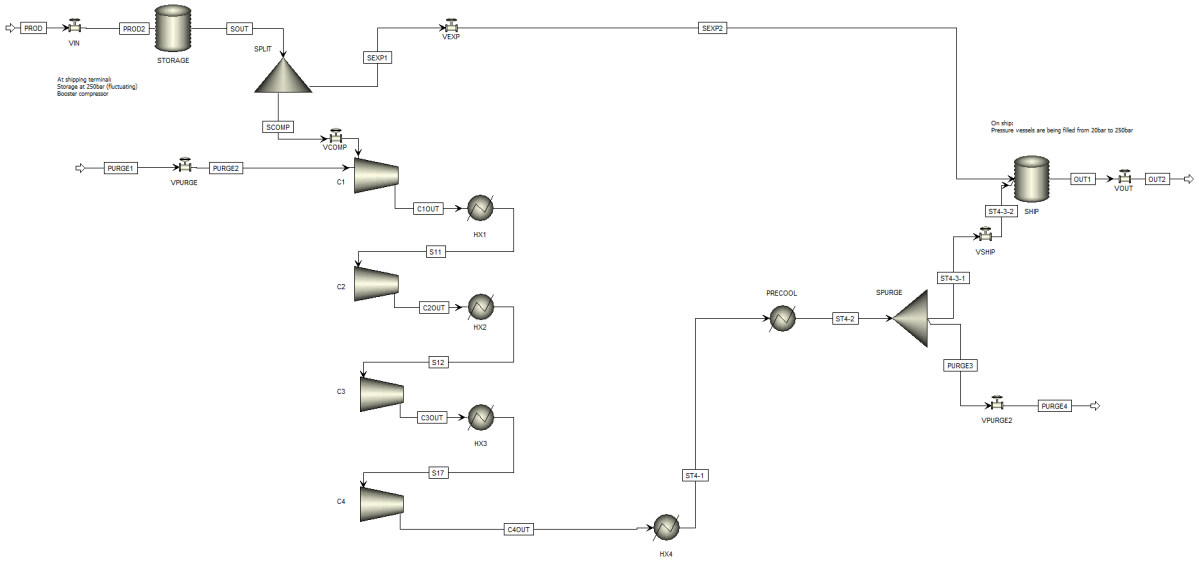

Figure 9: Process scheme for the loading infrastructure of a shipping terminal for cH_2 export

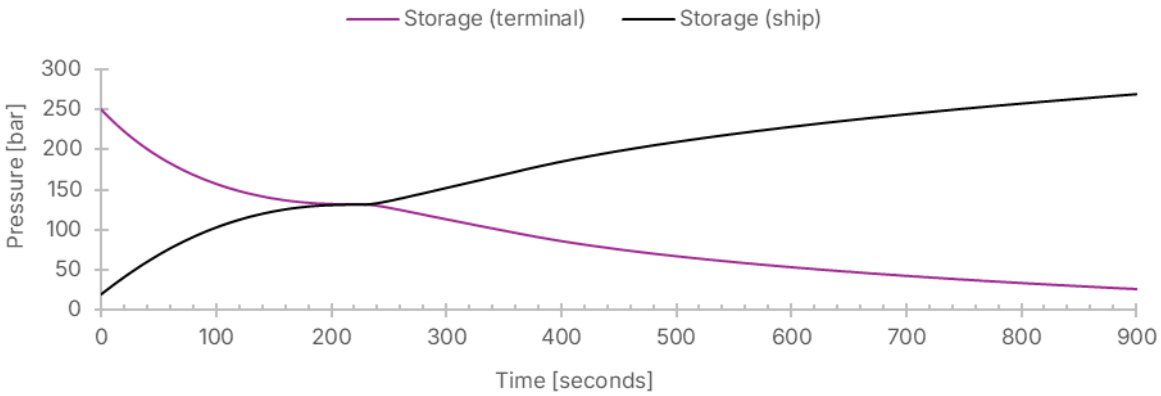

Figure 10: Timeline for the filling operation of a module in a cH_2 ship at the export terminal

Table 4: Shipping terminal for compressed hydrogen export – System description

Parameter	Value	Unit	Source

Investment cost factors – cH_2 Tube Trailer Terminal			
TASC Booster compressor	47.4	MNOK2024/bay	Calculation from section 3.1.5
TASC H_2 intermediate storage	21.95	kNOK2024/kg H_2	Calculation from section 3.6
Investment cost factors – Loading Infrastructure			
TASC Terminal construction (100 MW)	24.3	MNOK2024	Based on Songhurst [29]
TASC Booster compressor	134	MNOK2024	Calculation (400 modules, 800min filling time)
TASC Precooler	130	MNOK2024	Calculation (400 modules, 800min filling time)
Energy – cH_2 Tube Trailer Terminal			
Booster compressor electricity	0.35	kWh/kgH_2	Calculation from section 3.1.5
Energy – Loading Infrastructure			
Booster compressor electricity	0.37	kWh/kgH_2	Calculation
Precooler electricity	0.16	kWh/kgH_2	Calculation using COP=1.1 [25]
Cooling water for stage cooler	0.31	kWh/kgH_2	Calculation
Operating cost factors			
Electricity			Depending on price zone
Salary cost per staff	703.5	kNOK2024/a	Supplementary material, section 1.3.1
Maintenance	5	% of TPC	Assumption

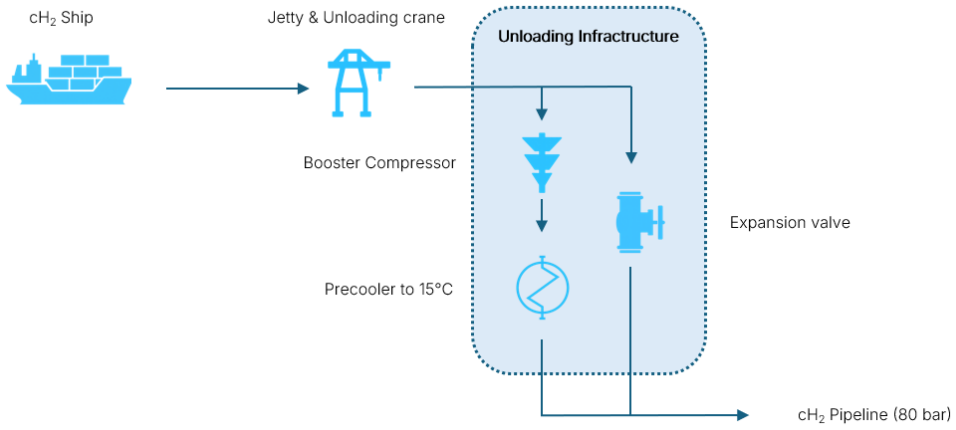

Figure 11: Process sketch of a shipping terminal for cH_2 import

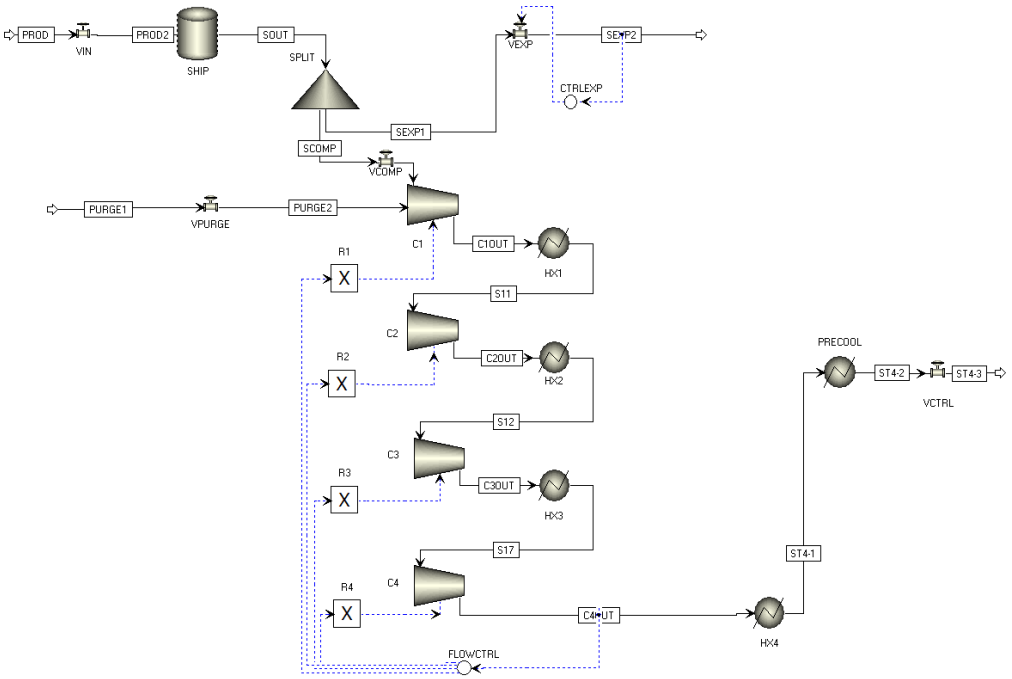

Figure 12: Process scheme for the unloading infrastructure of a shipping terminal for cH_2 import

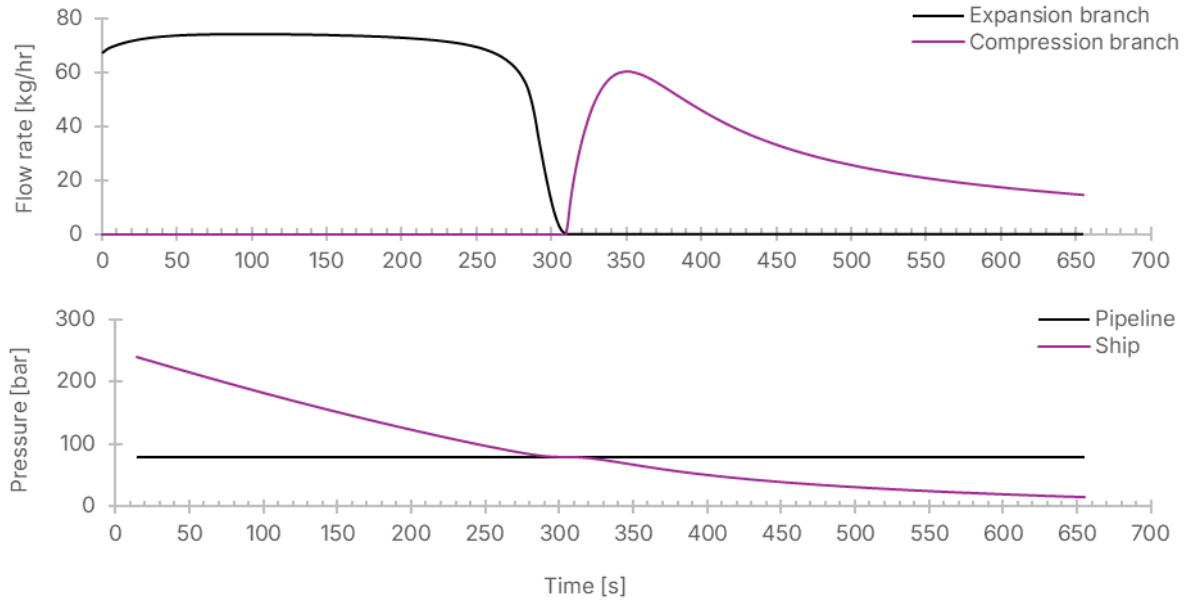

Figure 13: Timeline for the emptying operation of a module in a cH_2 ship at the import terminal

Table 5: Shipping terminal for compressed hydrogen import – Investment costs (100MW)

Parameter	Value	Unit	Source
Investment cost factors			
TASC Booster compressor	235	MNOK2024	Calculation using ship size of 400 modules and 200min emptying time
TASC Terminal construction (100 MW)	24.3	MNOK2024	Based on Songhurst [29]
Electricity demand	0.15	kWh/kgH_2	Aspen Dynamics
Operating cost factors			
Electricity price	78.5	EUR/MWh	Example, Bundesnetzagentur [31]
Salary cost per staff	703.5	kNOK2024/a	Supplementary material, section 1.3.1

Maintenance	5	% of TPC	Assumption

3.2.5. Trade-off on filling time

At the export terminal, there is a trade-off between equipment cost (*i.e.*, corresponding to the size of the booster compressor and the precooling unit) and transfer time. More modules being loaded in parallel requires larger equipment, resulting in higher investment costs for the terminal operator. At the same time, more modules loaded in parallel means less loading time per ship and thus less dead time costs at terminal for the shipping operator. We assumed that the terminal should be designed such that the total costs are minimized (see Eq 1), which is a compromise between shipping costs and terminal costs.

$$\mathbb{P}_{export\ terminal}(\boldsymbol{p} = \{\boldsymbol{n_{modules}}, \boldsymbol{m_{terminal}}, \boldsymbol{d_{route}}\}): \quad min_{t_{fill}}\ c_{terminal,export,inv}(n_{modules}, m_{terminal}, t_{fill}) + c_{ship}(n_{modules}, t_{fill}, d_{route}) \quad \text{Eq 1}$$

where $\mathbb{P}$ is the optimization problem solved as a function of parameter set $\boldsymbol{p}$. $n_{modules}$ is the number of modules on the cH_2 ship (see section 3.4), $m_{terminal}$ is the terminal throughput, d_{route} is the shipping distance and t_{fill} is the ship filling time.

$c_{terminal,export,inv}$ is the specific annualized investment cost of the export terminal, which includes the costs of the compressors and precooling unit, construction of the jetty, equipment lifetime and capital recovery factors, and is a non-linear continuous function of scale and rate. c_{ship} is the specific shipping cost, which includes annualized ship investment costs, operating costs, equipment lifetime and capital recovery factors, and is a linear continuous function of the transfer time. The shipping costs should be understood as the specific costs of a fully utilized ship on the given shipping route. Given the amount of hydrogen shipped, the actual utilization of ships in the fleet might be lower and thus shipping costs higher. The cost functions are defined in the Excel worksheet "Shipping.xlsx" provided in the supplementary material.

A graphical illustration of Eq 1 is depicted in Figure 14. Figure 14 was created assuming a one-way shipping distance of 580 km. The shipping distance influences the shipping cost and thus the absolute value of specific hydrogen costs but varying the one-way shipping distance between 200 km and 2000 km does not change the optimal filling time and thus terminal costs.

In general, there is a trend that longer filling times lead to lower overall costs. However, the maximum allowable filling time is defined by the terminal throughput and ship size. At this maximum allowable filling time, the intermediate storage demand becomes zero, resulting in a buckle in the graph. Filling times exceeding this value are physically not possible. For all investigated combinations of terminal throughput and ship size, the optimum terminal design is located at the maximum allowable filling time. Figure 22 shows where the position of this buckle moves with respect to terminal throughput and ship size.

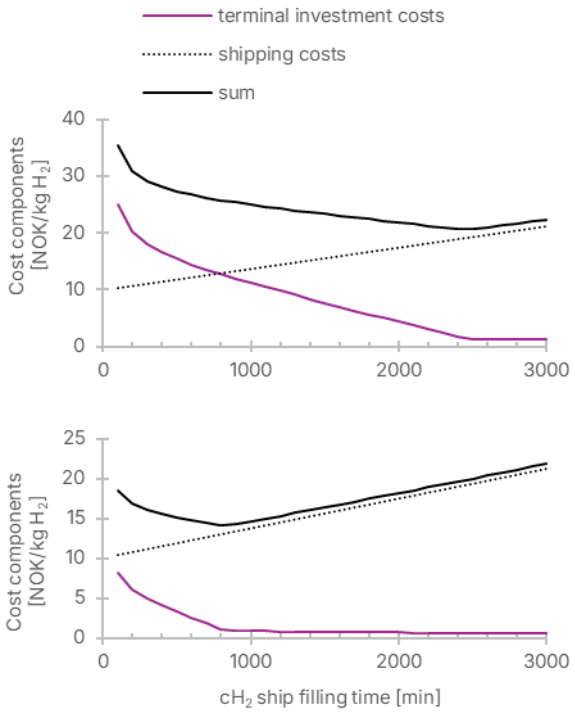

Figure 14: Dependency of export terminal cost on cH_2 ship filling time for a ship with 400 modules and a one-way shipping distance of 580km (throughput top: 100 MW, bottom: 300 MW)

3.3. Shipping terminal for compressed hydrogen shipping (import)

3.3.1. Terminal design

Figure 11 shows the conceptual design of a shipping terminal for the import of compressed hydrogen. On the receiving side, compressed hydrogen ships dock to the terminal. We assume a time loss of 30min for docking and undocking. As in the shipping terminal for compressed hydrogen export, the terminal has a single berth design. The maximum terminal throughput is thus directly linked to the size of the unloading equipment. We assume that the ship can directly unload into an 80-bar pipeline grid without the need for intermediate storage and without disturbing the pressure in the pipeline. Unloading requires an expansion valve for when the ship's pressure is higher than the pipeline pressure and a booster compressor for further unloading.

3.3.2. Model description

A model in Aspen Plus Dynamics using the PR-BM property package was built to model the emptying of one pressure vessel in the ship. We assume that the actual emptying process consists of c emptying cycles of n modules being emptied simultaneously. Thus, the total emptying time of a ship with n*c modules is calculated as the cycle time times the number of cycles c. The number of modules emptied

at the same time n is used as a linear factor to determine the size of the equipment.

The emptying operation consists of two phases. First, as long as the pressure level in the ship is larger than the pipeline pressure, the ship is emptied via an expansion branch. Herein, hydrogen flows through an expansion valve, which is opened at the start. The transfer time of the expansion branch is 309s. The second phase starts when the pressure in the ship drops to 80 bar. Then, a booster compressor is used to empty the ship down to the lower upper operational hydrogen density of 1.63 kg/m³ (*i.e.*, density at 20 bar and 20°C). The second phase starts when the expansion valve is closed. The compression valve is opened over 100s to avoid spikes in flow rate. The booster compressor has a 4-stage design with intermediate cooling to 20°C. The power of the booster compressor is controlled to achieve a set flow rate of 75 kg/hr per vessel. This means that if only one module is unloaded at a time, a flow of 100 MW hydrogen (LHV) is achieved, which was assumed as the minimum unloading rate. The controller can increase the power up to a maximum power level to achieve the flow rate set point. The model was run with different maximum set power levels, which resulted in different transfer times. The result of this analysis is stated in Figure 15, which states the total emptying time of a module depending on the power of the booster compressor. The timeline of the emptying operation is stated in Figure 13. After emptying, an adiabatic temperature of -40°C is reached in the pressure vessels in the ship. We assumed that 400 kW compressor power per module is a reasonable trade-off and used this value for further analysis.

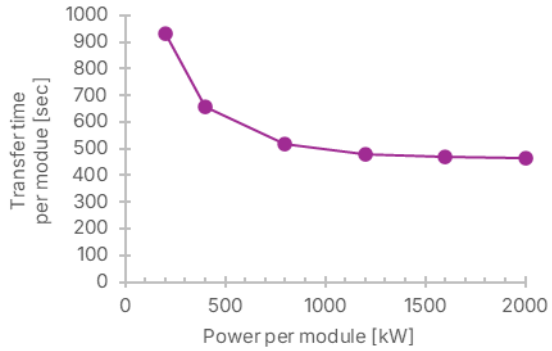

Figure 15: Trade-off for sizing of the booster compressor at compressed hydrogen import terminals

3.3.3. Cost calculation

Table 5 shows the investment cost factors for a hydrogen import terminal. The calculation for costs for terminal construction is equivalent to the export terminals. We assume a staff size of 4 workers. We assume that the lifetime of the terminal is 20 years.

Table 5 states the operating costs for the hydrogen import terminal. The average day ahead price in Germany in 2024 was used as the electricity price at the terminal. The salary calculation is identical to the export terminal (see Table 4). While the import terminal is not located in Norway, we assume that the terminal is operated by a Norwegian company for simplicity. Maintenance costs were assumed to be 5% of the TPC for the booster compressor. Port fees (*i.e.*, fees for entry and exit of a port) are taken from the Port of Wilhelmshaven [32] and are based on the gross tonnage of the ship.

3.3.4. Trade-off on emptying time

As in the export terminal, there is a trade-off between equipment size and transfer time. More modules being unloaded in parallel requires a larger booster compressor, resulting in higher investment costs for the terminal operator. At the same time, more modules unloaded in parallel means less unloading time per ship and thus less dead time costs at the terminal for the shipping operator. We assumed that the terminal should be designed such that the total costs are minimized (see Eq 2), which is a compromise between shipping costs and terminal costs.

Eq 2
$$\mathbb{P}_{import\ terminal}(\boldsymbol{p} = \{\boldsymbol{n_{modules}}, \boldsymbol{m_{terminal}}, \boldsymbol{d_{route}}\}):$$
$$min_{t_{empty}}\ c_{terminal,import,inv}(n_{modules}, m_{terminal}, t_{empty}) + c_{ship}(n_{modules}, t_{empty}, d_{route})$$

where $\mathbb{P}$ is the optimization problem solved as a function of parameter set $\boldsymbol{p}$. $n_{modules}$ is the number of modules on the cH_2 ship (see section 3.4), $m_{terminal}$ is the terminal throughput, d_{route} is the shipping distance and t_{empty} is the ship emptying time.

$c_{terminal,import,inv}$ is the specific annualized investment cost of the import terminal, which includes the costs of the compressors, construction of the jetty, equipment lifetime and capital recovery factors, and is a non-linear continuous function of scale and rate. c_{ship} is the specific shipping cost, which includes annualized ship investment costs, operating costs, equipment lifetime and capital recovery factors, and is a linear continuous function of the transfer time. As in section 3.2.5, the shipping costs should be understood as the specific costs of a fully utilized ship on the given shipping route. The cost functions are defined in the Excel worksheet "Shipping.xlsx" provided in the supplementary material.

A graphical illustration of Eq 2 is depicted in Figure 16. Figure 16 was created assuming a one-way shipping distance of 580km. The shipping distance influences the shipping cost and has thus a strong influence on the absolute value of specific hydrogen costs and a weak influence on the optimal filling time. However, varying the one-way shipping distance between 200km and 2000km showed only insignificant changes to the position of the optimum. Thus, we ignored the shipping distance as a parameter.

In general, there is a trend that the optimal emptying time decreases with increasing terminal throughput and increases with increasing ship size. At the import terminal, the equipment size and thus the annualized terminal investment cost is dependent on both the ship size and the terminal throughput. Increasing terminal throughput and increasing ship size leads to larger optimal equipment sizes and thus

larger terminal investment costs. Figure 23 shows where the position of the optimum moves with respect to terminal throughput and ship size.

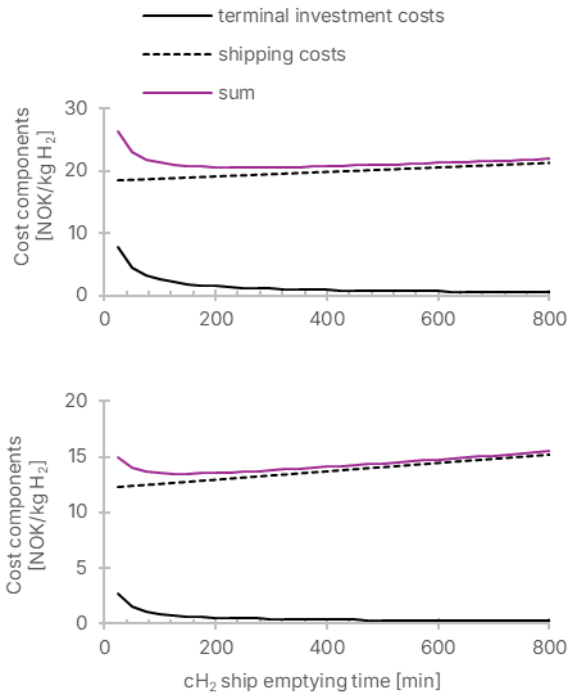

Figure 16: Dependency of import terminal cost on cH_2 ship emptying time for a ship with 400 modules and a one-way shipping distance of 580km (throughput top: 100 MW, bottom: 300 MW)

3.4. Ship for transport of compressed hydrogen

3.4.1. Ship design

Table 7 states the system design for a theoretical compressed hydrogen ship. The concept for the ship is based on d'Amore *et al.* [9]. The study suggested a modular design for the ship, based on shipping containers (i.e., modules) which are stacked with 40 pressure vessels each. A ship has hundreds of these modules on board and could thus be in principle constructed in a similar way as a container ship. As a standard assumption, we used a ship with a size of 400 modules, as the specific costs do not decrease significantly beyond that for a transport distance typical for southern Norway to northern Europe (see Figure 19). The actual number of modules on board has a strong influence on shipping costs and should be optimized for the used supply chain (see Eq 3). The nominal operational pressure of the hydrogen pressure vessels was set to 250 bar, but we assume that slight overfilling is allowed.

The vessels were assumed to be type IV pressure vessels made of a composite material with a material density of 1350 kg/m^3 and a tensile strength of 1200 MPa. For the calculation of the wall thickness, the relation stated in ASME BPVC.VIII.1-2015 UG27 was used combined with a safety factor of 2.35 [12]. The number of modules stacked in the ship has a significant impact on economic feasibility and should be optimized for the actual shipping route where the ship would be deployed. The deadweight tonnage was approximated as the weight of all modules (i.e., cargo weight). The gross tonnage was correlated from the deadweight tonnage based on real data from 45 general cargo and tanker ships sourced from Marine Traffic. It should be noted that these values are only correlated with an R^2 of 0.77, meaning that the gross tonnage has high uncertainty. The gross tonnage is however only used for the calculation of port fees, which have a low share in total cost. The payload is calculated based on the upper operation density (at 250 bar and 20°C) minus the lower operational density (at 20 bar and 20°C).

3.4.2. Cost calculation

The cost of the empty ship (*i.e.*, a ship without hydrogen storage modules) was calculated using the correlations for a general cargo sip from Mulligan [33] adjusted with the PPI for ship building (PCU3366133661). The cost for the pressure vessels was calculated as the average of two literature values. Reddi et al. [12] reported 25 $2018/lb composite material for material and manufacturing. On the other hand, Houchins et al. [34] reported a cost of 12 $2021/kWh hydrogen (LHV) for a 350 bar pressure vessel with little sensitivity to nominal pressure. While the value was stated for long-haul truck transport, we assume that it is also valid in this context. The cost of a module consists of the cost of the pressure vessels multiplied by an assumed installation factor of 1.1 for piping, hydrogen leakage monitoring equipment and installation plus the cost of the empty container.

We assume that the ship is manned by a staff of 20, consisting of 10 ship's machinists and 10 deck operators. Respective average salaries in these occupational groups were taken from SSB [30]. Variable OPEX consist of port fees and fuel costs. A trip is defined as a journey starting with an empty ship at the export terminal, loading the ship with hydrogen, sailing to the destination, unloading at the import terminal, and returning to the export terminal.

We assumed a sailing speed of 20 knots, which is common for cargo ships [35]. The fuel consumption during sailing was estimated based on the deadweight tonnage and speed using the regression from Cepowski et al. [35] and cross-validated using data from Rohner [36] for a sailing speed of 15 knots. It should be noted that the fuel consumption is subject to high uncertainty. The fuel consumption calculation is based on deadweight tonnage, which might not correlate with the actual ship's size in the same way as it does for common cargo ships, since the density of the cargo is rather low (see Table 7, module weight). However, the fuel costs are only a small part of the total transport costs.

The fuel consumption during loading and unloading times at terminal was assumed to be 5% of the nominal fuel consumption. A fuel price of 5.67 kNOK2024/tonne was used, which is the average

price for VLSFO in Rotterdam between September 13, 2024 and March 12, 2025 [37]. We further assume a calendar lifetime of 20 years for the ship and pressure vessels and a cycle lifetime of 20 000 cycles.

3.4.3. Specific shipping costs

3.4.3.1. Pressure dependency

There is a slight dependency of shipping costs on nominal pressure. While the payload increases with increasing pressure, this relation weakens at higher pressures. On the other hand, costs increase linearly with increasing pressure. This leads to the creation of an optimal nominal pressure, which is dependent on the ship's size. However, this also means that the ship size can be optimized given a fixed nominal pressure. In that manner, the nominal pressure can be eliminated as a decision variable.

3.4.3.2. Dependency on design parameters

Figure 19 shows the specific costs of a cH_2 ship as a function of one varied parameter while holding the other key parameters fixed. It can be seen that the two most influential parameters on specific shipping costs are shipping distance and ship size. There is a linear increase in specific shipping costs with shipping distance if other parameters are held fixed. Increasing ship size leads to a logarithmic decrease of specific shipping costs. However, larger ship sizes also lead to higher terminal costs if terminal transfer times are held fixed. Moreover, there is also a linear correlation between specific shipping costs and terminal time and ship utilization.

3.4.3.3. Comparison with literature

There are only few studies in literature that consider shipping of compressed hydrogen. Table 6 compares literature values for cH_2 shipping costs with costs that were computed using our model with parameters for ship size and shipping distance as reported in the literature. We assume further a utilization of 8400h/a, 960 min/trip terminal time and if not stated, a shipping distance of 1000 km/trip. Cost values reported in literature were time-adjusted using the Producer Price Index for Ship and Boat Building (PCU3366133661) and currency adjusted using average 2024 exchange rates.

Babarit et al. [10] assumed a ship with 700 bar design pressure and 150 tonnes payload. They reported a specific shipping cost of 0.54 EUR2018/kg H_2 for a one-way shipping distance of 1000km, which translates to 7.8 NOK2024/kg H_2. d'Amore-Domenech [9] assumed a design pressure of 200 bar and a payload of 2000 tonnes. The study assumed further a charter rate of 95 kUSD/d, which they derived from a LH_2 ship concept. With the above-mentioned assumptions, this translates into specific shipping costs of 1.1 NOK/kg H_2. Cebolla *et al.* [5] conducted a thorough analysis of hydrogen delivery options, assuming a compressed hydrogen ship operating at 250 bar with a payload of 1245 tonnes. The study states a sensitivity of costs over shipping distance, which we used to find the literature costs for a 1000 km/trip shipping distance (i.e., 500km one-way).

Table 6: Comparison of shipping cost with literature

Reference	Size *modules*	Literature *NOK/kg H_2*	Our study *NOK/kg H_2*
Babarit et al. [10]	486	7.8	17.9
d'Amore-Domenech et al. [9]	6475	1.1	7.4
Cebolla et al. [5]	4031	5.2	7.6

3.4.4. Trade-off on total shipping costs

For the cH_2 ship, there is a trade-off on ship size (i.e., number of modules). If the terminal times are set as a fixed value independent of ship size, increasing ship size leads to lower specific shipping costs due to economies of scale (see Figure 19). On the other hand, we showed in section 3.2.5 and section 3.3.4 that both optimal filling time and optimal emptying time are a function of ship size. Increasing ship size leads to longer filling times at the export terminal (see Figure 22) and longer emptying times at the import terminal (see Figure 23). This in turn leads to higher dead-time costs for shipping, which contributes to an increase in shipping costs. Moreover, the terminal investment costs are affected by an increase in transfer times and ship size. We assume that the ship should be sized such that the total shipping cost is minimized (see Eq 3). The total shipping cost is the sum of specific annualized terminal investment costs and specific shipping costs. The terminal operating costs are left out of the optimization problem since they would only constitute a constant offset in the total shipping costs and not change the position of the optimum.

Eq 3
$$\begin{aligned}&\mathbb{P}_{ship}(\boldsymbol{p} = \{\boldsymbol{m_{route}}, \boldsymbol{d_{route}}\}):\\ &min_{n_{modules}}(c_{terminal,export,inv,opt}(m_{route})\\ &+ c_{terminal,import,inv,opt}(m_{route}, n_{modules})\\ &+ c_{ship}(n_{modules}, d_{route}))\end{aligned}$$

where m_{route} is the route throughput, d_{route} is the shipping distance, $n_{modules}$ is the number of modules on the ship, $c_{terminal,export,inv,opt}$ is the specific annualized investment cost of a export shipping terminal which has optimal size (i.e., optimal solution to problem Eq 1), $c_{terminal,import,inv,opt}$ is the specific annualized investment cost of a import shipping terminal which has optimal size (i.e., optimal solution to problem Eq 2) and c_{ship} is the specific shipping costs of a fully utilized ship with a size of $n_{modules}$ which is employed on a route with a shipping distance d_{route}. We hereby assume that the hydrogen throughput of the shipping route is identical to the hydrogen throughput of the terminals. The problem Eq 3 was solved using the reduced models described in section 4.2 and 4.3 to calculate the optimal solution to Eq 1 and Eq 2. Eq 6 and Eq 8 were used to calculate the terminal transfer times given the ship size, shipping distance and route throughput. The specific annualized terminal investment costs are a direct function

of transfer times. The cost functions are defined in the Excel worksheet "Shipping.xlsx" provided in the supplementary material.

A graphical illustration of Eq 3 is depicted in Figure 17. Figure 17 shows an example of the problem for a shipping distance of 1160 km/trip and a route throughput of 100 and 300 MW. While Figure 19 suggests a general cost reduction with increasing ship size given fixed terminal times, it can be seen from Figure 17 that increasing ship size does not generally lead to lower total shipping costs. This situation arises due to optimized terminal times, which increase with increasing ship sizes (see Figure 22 and Figure 23) and thus increase total shipping costs.

In general, this leads to an optimum ship size as a function of shipping distance and amount of hydrogen shipped. Figure 21 shows how the position of this optimum moves with changing input parameters. However, it should be noted that the function is quite flat around the optimum and a non-optimal ship size might only increase total costs insignificantly. For example, for a shipping distance of 1160 km/trip and a route throughput of 300 MW leads to an optimal ship size of 500 modules and a "sum" of 14.65 NOK/kg H_2. However, choosing a ship size of 400 modules would lead to a "sum" of 14.76 NOK/kg H_2, increasing the supply chain costs by 0.7%.

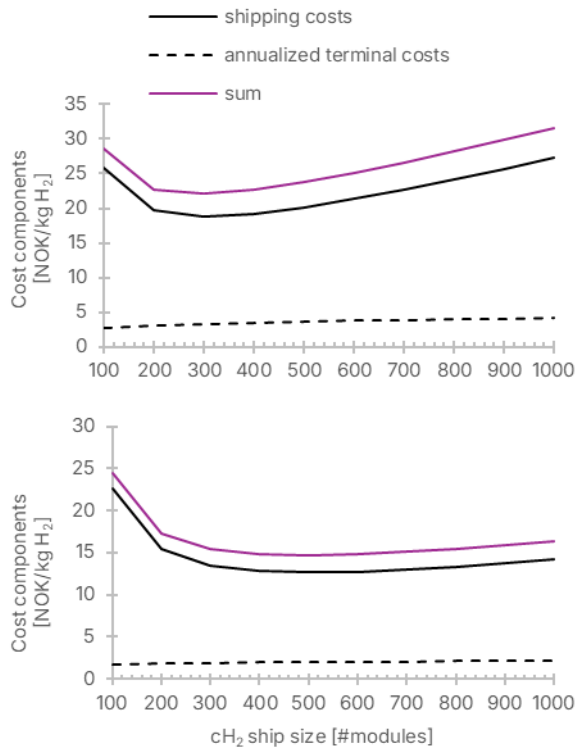

Figure 17: Dependency on supply chain costs on cH_2 ship size for a one-way shipping distance of 580km and 100 MW (top) or 300 MW (bottom) hydrogen throughput given optimal terminal times

3.4.5. Fleet costs

Figure 18 shows the specific fleet costs of a fleet of identical cH_2 ships (i.e., 400 modules, 960 min/trip terminal time, 8400 hours maximum utilization) as a function of fleet size. With increasing hydrogen throughput, more ships are required, resulting in jumps in the specific cost curve. On the other hand, the utilization of the fleet increases with increasing hydrogen throughput, lowering the specific costs. It is evident that the actual fleet costs always exceed the specific costs of a single fully utilized ship, unless all ships in the fleet are fully utilized. Larger fleets are less sensitive to this issue, as the risk of underutilization is spread across the entire fleet.

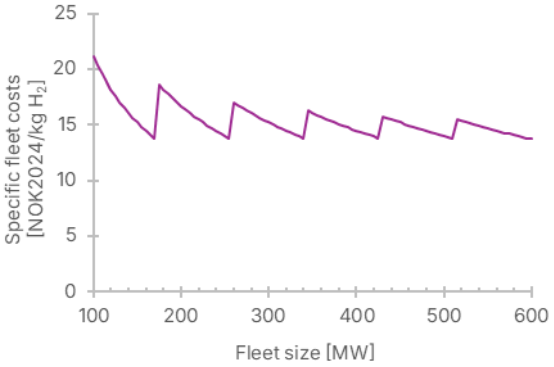

Figure 18: Specific cH_2 shipping costs as a function of fleet size.

Table 7: Ships for compressed hydrogen transport – System description

Parameter	Value	Unit	Source
Pressure vessel description			
Nominal pressure	250	bar	Assumption, see discussion below

Vessel outer radius	295	mm	Based on d'Amore et al. [9]
Vessel height	2.15	m	Based on d'Amore et al. [9]
Vessel wall thickness	14.3	mm	ASME BPVC.VIII.1 - 2015 UG27
Vessel weight	75.2	kg	Estimate based on cylinder volume
Module description			
Number of H_2 vessels per module	40		Assumption from d'Amore et al. [9]
Container weight	2300	kg	Assumption
Module total weight	6.5	t	Calculation (excluding stored H_2)
Module container cost	100	kNOK2024	Assumption
Module total cost	2277	kNOK2024	Calculation
H_2 Payload per module (useful)	317.8	kg	Calculation
Ship description			
Number of modules	400	-	Assumption
Deadweight tonnage	2263	t	Calculation
Gross tonnage	1591	-	Estimate from deadweight
Ship Investment costs (400 modules)			
Cost of bare ship	203	MNOK2024	Calculation based on Mulligan [33]
Cost of modules	911	MNOK2024	Calculation, see Table 7
Fixed OPEX			
Number of staff	20	-	Assumption
Salary costs	23.7	MNOK2024/a	Supplementary material, section 1.3.1
Maintenance	33.4	MNOK2024/a	Assuming 3% of ship's costs
Insurance	10	MNOK2024/a	Assumption
Variable OPEX (400 modules)			
Fuel consumption during sailing	36.3	t/day	Calculation based on Cepowski et al. [35]
Fuel consumption at terminal	1.81	t/day	Assumption (5% fuel consumption)
Ship Operation			
Lifetime	20	a	Assumption
Utilization	8400	h/a	Assumption based on Roussanaly [38]

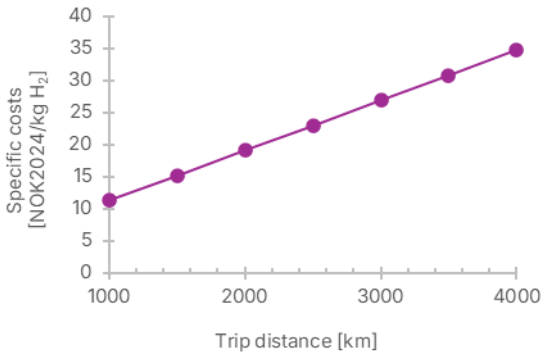

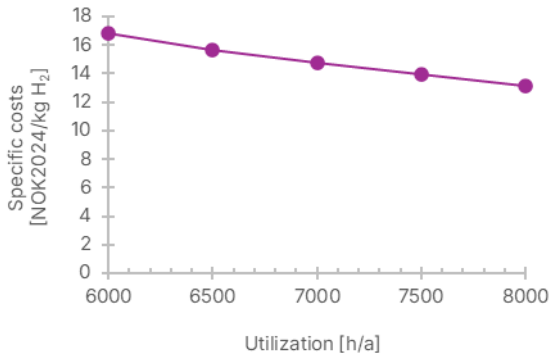

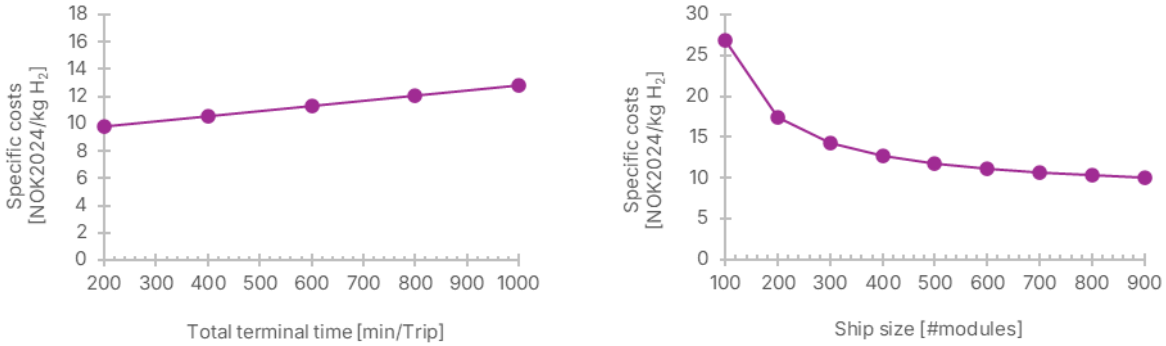

Figure 19: Sensitivity of cH_2 shipping costs varying one parameter (standard assumptions: 1160km trip distance, 8400 hours annual utilization, 960 min/trip terminal time, ship size of 400 modules)

3.5. Hydrogen compression

We modelled investment cost and energy consumption for hydrogen compression using the correlations reported by Khan et al [27]. Herein, we used the system using large centrifugal compressors as the baseline. We assumed that the compressors are driven by electric motors with an efficiency of 95%, an isentropic compressor efficiency of 80% and a compressor lifetime of 15 years.

3.6. Compressed hydrogen storage

Many hydrogen production and distribution operations require intermediate hydrogen storage to ensure continuous operation. For high pressure intermediate storage, we assume pressure vessels grouped into larger modules of 40 pressure vessels each, such as in compressed hydrogen shipping modules (see section 3.4).

Necessary wall thicknesses were calculated using Barlow's formula with a safety factor of 3. We assumed a SA-372 Grade J, Class 70 steel with a material density 7667 kg/m^3 and a tensile strength of 827.4 MPa and a specific cost of 3.5 USD2018 per lb of steel [12].

4. Reduced models

Starting with the detailed models, reduced models were made that have characteristics that are suitable for use as a part of a large, complex model in a supply chain optimization framework with many equations and variables. Specifically, the models should be linear or piecewise linear, convex, and reasonably accurate within the range of intended use. Models that cannot be reduced into this format while retaining accuracy should be left in their more complex form.

4.1. cH_2 Tube Trailer

Figure 20 shows the relation between driving distance and costs for a cH_2 tube trailer as derived in section 3.1.2. We hereby assume that the tube trailer is employed on a fixed route between a hydrogen production facility and a hydrogen shipping terminal.

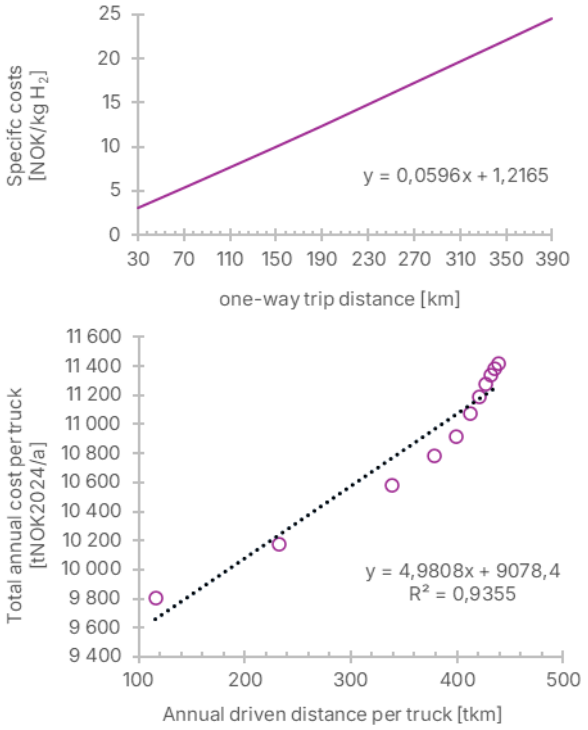

Figure 20: Relation between driving distance and cost for a cH_2 tube trailer (top: specific cost, bottom: total annual cost

4.2. cH_2 shipping terminal (export)

Figure 22 shows the relationship between optimal export terminal investment costs as well as optimal ship filling time and terminal throughput as derived in section 3.2.5. Every point in Figure 22 is the solution of the problem stated in Eq 1 given the ship size and terminal throughput. The equation Eq 5 for the terminal investment costs was determined by linear regression, which achieved a R^2 of 0.99. The equation Eq 6 for optimal filling time was derived analytically as the maximum allowed filling time given the terminal throughput and ship size. The average terminal throughput in kg/min has to be translated from the average terminal throughput in MW. The offset of 30 minutes accounts for the time loss for docking and undocking.

It can be seen that the optimal annualized terminal cost is independent of ship size. This situation

arises because all combinations of ship size and terminal throughput lead to a filling time which is such that the filling rate in Megawatts is equal to the respective terminal throughput, eliminating the need for large-scale intermediate storage at the export terminal. This shows that it is more economical to have time-inefficient shipping (i.e., large terminal dead times) than intermediate hydrogen storage. For the same terminal throughput, larger ships lead to larger filling times, resulting in the same filling rate in Megawatts. With increasing terminal throughput, it becomes more economical to invest in larger equipment, decreasing filling times and thus decreasing the ship's dead time costs.

4.3. cH_2 shipping terminal (import)

Figure 23 shows the relationship between optimal import terminal investment costs as well as optimal ship emptying time and terminal throughput as derived in section 3.3.4. Every point in Figure 22 is the solution of Eq 2 given the ship size and terminal throughput. While the relationship between optimal emptying time and terminal throughput is not strictly linear, the total cost curve is very flat around the optimum (see Figure 16). A small error in the prediction of optimal emptying time does thus not significantly influence the total shipping costs. Thus, we assumed that a linear regression is an appropriate representation of Figure 23. The regression equations are stated in the equations Eq 7 and Eq 8 and achieve an R^2 of 0.96 and 0.87, respectively.

4.4. cH_2 ship size

Figure 21 shows the relationship between optimal cH_2 ship size and hydrogen throughput as well as shipping distance as derived in section 3.4.4. Based on this relation, we conducted a linear regression, which is stated in Eq 4 and achieved an R^2 of 0.94.

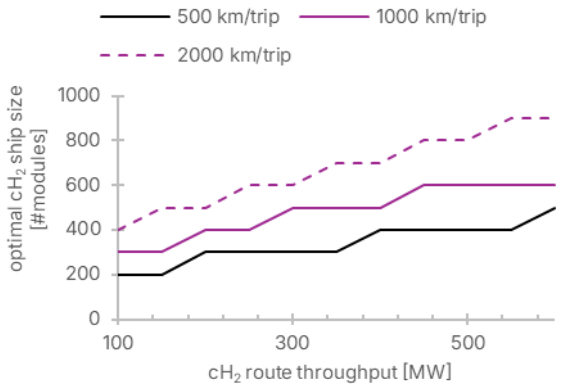

Figure 21: Optimal cH_2 ship size as a function of cH_2 throughput and shipping distance

Eq 4

$$n_{modules,opt}\ [\#\ modules] = + 0.733 \cdot m_{route}\ [MW] + 0.219 \cdot d_{route}\ [km/trip] - 15.76$$

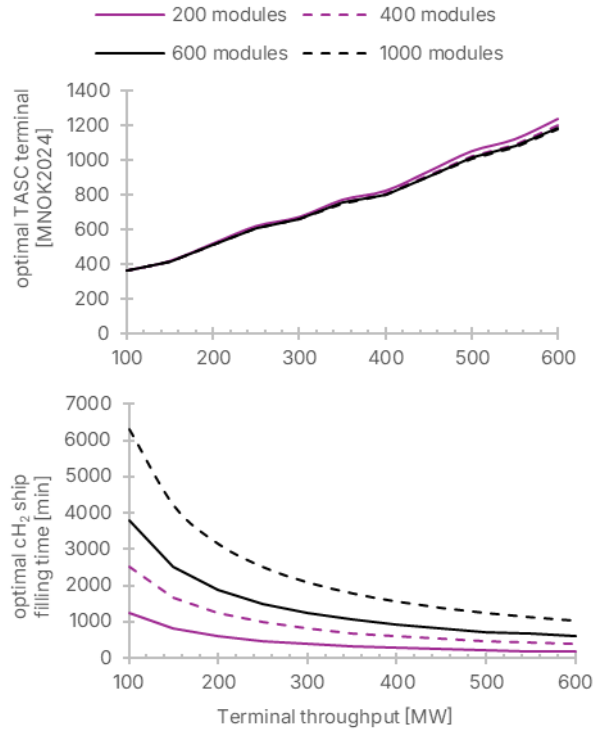

Figure 22: Export terminal design as a function of terminal throughput and ship size

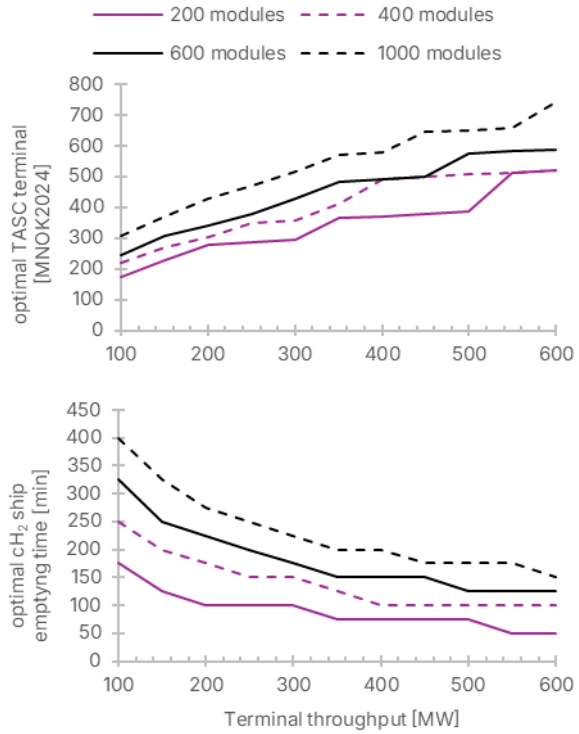

Figure 23: Import terminal design as a function of terminal throughput and ship size

Eq 5
$$c_{terminal,export,inv,opt}\ [MNOK2024] = + 1.64 \cdot m_{terminal}\ [MW] + 197.1$$

Eq 6
$$t_{fill,opt}\ [min] = n_{modules}\ [\#modules] * m_{module}\ [kg\ H_2/module] : m_{terminal}\ [kg\ H_2/min] - 30$$

Eq 7
$$c_{terminal,import,inv,opt}\ [MNOK2024] = + 0.694 \cdot m_{terminal}\ [MW] + 0.24 \cdot n_{modules}\ [\#\ modules] + 59.5$$

Eq 8
$$t_{empty,opt}\ [min] = - 0.311 \cdot m_{terminal}\ [MW] + 0.173 \cdot n_{modules}\ [\#\ modules] + 175.3$$

4.5. Total shipping costs

Combining all equations and setting terminal times as well as ship size to their optimal values given hydrogen throughput and shipping distance, the minimum total shipping cost can be calculated. This relationship is stated in Figure 24, which shows the total shipping costs for different situations. The costs include annualized investment costs for shipping terminals and shipping costs. Depending on the actual location of the shipping terminals, the operating costs have to be calculated and added to the total costs as a constant offset. They might be different for different terminals due to location dependent electricity prices. Note that the shipping costs represent the cost of a fully utilized ship. Depending on the number of ships in the fleet, the actual ship utilization might be lower and thus the specific shipping costs higher.

It can be seen that the supply chain costs increase linearly with shipping distance and decrease logarithmically with hydrogen throughput. This is because increasing the route throughput, larger ships become more economical, leading to an overall cost reduction.

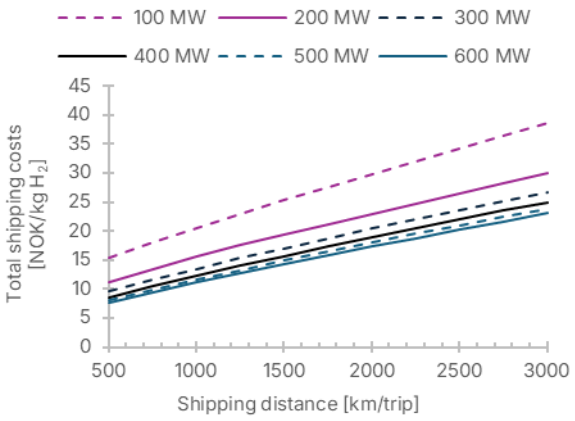

Figure 24: Total shipping costs as a function of shipping distance and hydrogen throughput

5. Conclusion

5.1. Alternative terminal design

It could be argued that the modular ship design would allow for swapping of the modules at the loading and unloading terminals instead of transferring the gas as proposed in Figure 8 and Figure 11. This would avoid the losses associated with the transfer of the gas to the intermediate storage at the export terminal and the transfer from the intermediate storage to the storage on the ship. The trade-off is that the time it takes to both load and unload the modules by crane at the import terminal is longer than the time required for gas transfer using compressors and that additional investment into modules at the import terminal would be required.

While theoretically possible, moving modules by crane is inferior to the transfer operations investigated in this study. For an example supply chain with 300 MW hydrogen throughput, 580 km one-way shipping distance and a ship size of 400 modules, the optimal filling time (i.e., the solution to problem Eq 1) is equal to the maximum possible filling time of 817 minutes, and the optimal emptying time (i.e., the solution to problem Eq 2) amounts to 151 minutes. Assuming the transfer operations investigated in this study, the shipping cost factors are 1.94 NOK/kg H_2 for terminal investment and 14.8 NOK/kg H_2 for shipping.

For container swapping, it is reasonable to assume a swapping time of 2 minutes per module [39] and two cranes operating in parallel. In the best case, modules could be simultaneously loaded and unloaded to and from the ship. This would lead to a transfer time of 800 minutes per ship at both terminals. At the export terminal, full modules from arriving tube trailers could be directly swapped with empty modules from the ship. There would be no need for compressors and precooling equipment at the export terminal. Hence, the investment costs could be reduced by 70%, leading to a cost reduction of 0.9 NOK/kg H_2. This is a best-case value since it assumes that there are no additional costs for swapping containers. The transfer time at the export terminal would be similar to the previously used value, having little influence on shipping costs.

At the import terminal, the transfer time would have to be increased from 151 minutes to 800 minutes, increasing the dead time costs for shipping by 2.4 NOK/kg H_2. The import terminal would still need the same equipment, since the unloading operation from the modules into the pipeline remains the same, with the only difference that the modules are emptied on land rather than directly from the ship. Since the ship empties into a pipeline system at the import side rather than tube trailers, there would also be a need for a storage of empty modules at the import terminal which can be swapped with full ones from arriving ships. At the bare minimum, an additional investment of 911 MNOK on modules would be required, translating to 1.7 NOK/kg H_2. All together, the total costs would increase by 3.2 NOK/kg H_2.

Moreover, this ignores the practical feasibility of

container swapping. Assuming a minimum swapping time of 2 minutes per module, the maximum terminal throughput is limited to 300 MW. Higher terminal throughputs would require either four cranes operating simultaneously or a second berth and two ships loading or unloading at the same time. Furthermore, using non-swappable fixed containers on the ship, there are no moving parts in the ship's cargo space and thus comparably low risk for sparks. On the other hand, loading and unloading containers filled with compressed hydrogen arguably leads to higher explosion risk given risk of sparks and falling containers.

5.2. General

We have found that the size of a cH_2 ship should be optimized given the transport distance and the estimated hydrogen throughout. Given the size of the cH_2 ship and hydrogen throughput, transfer times leading to the lowest total shipping costs can be found. For a complete estimate of supply chain costs, operating costs for the shipping terminals must be calculated and added to the costs stated in Figure 24.

For the design of the shipping modules, we assumed a lower design pressure of 20 bar. Increasing the lower design pressure would decrease the transfer times and thus decrease the absolute shipping costs. However, this would also decrease the payload and thus increase the specific shipping costs. Further research should be done on the importance of the lower design pressure and the net effect of increasing the parameter.

At shipping terminals, the optimal equipment size is in general a function of terminal throughput and ship size. However, at the export terminal, the optimal equipment size is independent of ship size, as the optimum filling time is always such that the filling power is equal to the average terminal throughput. We showed that it is economically beneficial to have large dead times at the export shipping terminals rather than building intermediate hydrogen storage (see section 3.2.5). This requires however a fleet size of at least two ships, since there must always be one ship sitting at the export terminal. The investigated trade-off minimizes the sum of shipping costs and terminal costs, resulting in a global minimum of the supply chain costs. In a real-world scenario, where multiple terminals are built by different companies and multiple ships are operated by different shipping companies, a different equilibrium might be reached. To find this equilibrium, a game-theoretical approach should be applied. The magenta line in Figure 14 plus a constant offset for operating costs would then illustrate the minimum rate a terminal operator has to charge for filling a cH_2 ship based on the equipment size.

As for import shipping terminals, we assumed that the terminal is perfectly connected to a hydrogen grid which can take up the imported hydrogen, eliminating the need for intermediate storage. This assumption might have to be challenged when the actual grid capacity is known, as the rate of hydrogen fed to the grid can be a multiple of the average hydrogen throughput. The shorter the emptying time, the higher the flow will rate spike. For example, a ship with 400 modules and an average terminal throughput of 300 MW translate to an optimal emptying time of 151 minutes. This would lead to a hydrogen flow of 2100 MW during unloading, which is seven times the average terminal throughput.

In addition to these conclusions about tradeoffs and decisions that should be made when designing a compressed hydrogen supply chain network, we also provided a collection of models that can be used for large scale supply chain optimization problems or for detailed design and operation considering process dynamics and transients. Modelers can choose the form of the model that best suits the nature of the problem and then apply them to the design of hydrogen supply chain networks in general. Most supply chain network problems are very case dependent based on important factors concerning geography, transportation networks, location, government policy, and markets, among others. This is left to future work, but the models can be used generally for many kinds of problems. The models have been made available to the general public via LAPSE at the links at the end of the article.

Declaration of symbols

c_{ship}	Shipping costs (only cH_2 ship)
$c_{terminal,export,inv}$	Investment cost for an export shipping terminal
$c_{terminal,export,inv,opt}$	Investment cost for an export shipping terminal which has optimal size following Eq 1
$c_{terminal,import,inv}$	Investment cost for an import shipping terminal
$c_{terminal,import,inv,opt}$	Investment cost for an import shipping terminal which has optimal size following Eq 2
d_{route}	Distance of the shipping route
m_{route}	Hydrogen throughput (route)
$m_{terminal}$	Hydrogen throughput (terminal)
$n_{modules}$	Number of modules on the ship
$n_{modules,opt}$	Optimal number of modules on the ship following Eq 3
t_{empty}	Emptying time of a ship at an import shipping terminal
$t_{empty,opt}$	Emptying time of a ship at an import shipping terminal which has optimal size following Eq 2
t_{fill}	Filling time of a ship at an export shipping terminal
$t_{fill,opt}$	Filling time of a ship at an export shipping terminal which has optimal size following Eq 1

Data transparency

The supplementary material states general assumptions on project economics and financing,

methodology on capital cost estimation and costs assumptions. The document draws on sources [21, 23, 30, 40-47]. The Aspen Plus Dynamics models developed for this work can be found in the Living Archive for Process Systems Engineering (LAPSE) at:

https://PSEcommunity.org/LAPSE:2025.0722

Acknowledgements

This project was funded by the NTNU-MIT Energy Research Programme (project NMERP-C1).

References

1. Guan, D., et al., *Hydrogen society: from present to future.* Energy & Environmental Science, 2023. 16(11): p. 4926–4943.
2. Hjorth, R. and A.M. Rustad, *Norway's 300 GW offshore wind opportunity*. 2023, BCG.
3. *Hva er utbyggingspotensialet for fornybar energi på land i Norge?* Veileder for økt fornybar energiproduksjon 2025-10-30]; Available from: https://innlandetfylke.no/tjenester/klima-energi-og-miljo/energi/veileder-for-okt-fornybar-energiproduksjon/4-hva-er-utbyggingspotensialet-for-fornybar-energi-pa-land-i-norge/.
4. Reuters. *Norway's Equinor scraps plans to export blue hydrogen to Germany*. 2024 2025-10-30]; Available from: https://www.reuters.com/business/energy/norways-equinor-scraps-plans-export-blue-hydrogen-germany-2024-09-20/.
5. Cebolla, O., D. F., and W. E., *Assessment of Hydrogen Delivery Options*. 2022, Joint Research Centre (JRC).
6. Peecock, A., et al., *Techno-economic assessment of liquid carrier methods for intercontinental shipping of hydrogen: A case study.* International Journal of Hydrogen Energy, 2024. 94: p. 971–983.
7. Kim, S., S. Oh, and S. Kang, *Techno-economic assessment of liquefied hydrogen tanker ships utilizing various propulsion systems.* Energy Conversion and Management, 2025. 336.
8. Ustolin, F., A. Campari, and R. Taccani, *An Extensive Review of Liquid Hydrogen in Transportation with Focus on the Maritime Sector.* Journal of Marine Science and Engineering, 2022. 10(9).
9. d'Amore-Domenech, R., et al., *On the bulk transport of green hydrogen at sea: Comparison between submarine pipeline and compressed and liquefied transport by ship.* Energy, 2023. 267.
10. Babarit, A., et al., *Techno-economic feasibility of fleets of far offshore hydrogen-producing wind energy converters.* International Journal of Hydrogen Energy, 2018. 43(15): p. 7266–7289.
11. Nekså, P., *MEDIUM SCALE DISTRIBUTION CHAINS FOR HYDROGEN*, in *The International Workshop of Energy Conversion*. 2023: Kyoto, Japan.
12. Reddi, K., et al., *Techno-economic analysis of conventional and advanced high-pressure tube trailer configurations for compressed hydrogen gas transportation and refueling.* International Journal of Hydrogen Energy, 2018. 43(9): p. 4428–4438.
13. *VDI Heat Atlas*. 2010.
14. Zhao, L., et al., *Thermodynamic analysis of the emptying process of compressed hydrogen tanks.* International Journal of Hydrogen Energy, 2019. 44(7): p. 3993–4005.
15. Couteau, A., P. Dimopoulos Eggenschwiler, and P. Jenny, *Heat transfer analysis of high pressure hydrogen tank fillings.* International Journal of Hydrogen Energy, 2022. 47(54): p. 23060–23069.
16. Vegvesen, S., *Normaltransport – Utdrag fra forskrift om bruk av kjøretøy kap. 5*. 2023.
17. Koshelkov, I., *Evaluation of mid-scale hydrogen distribution chains for compressed hydrogen*, N.U.o.S.a. Technology and D.o.E.a.P. Engineering, Editors. 2022.
18. Maes, M., et al., *IPHE regulations codes and standards working group - Type IV COPV round robin testing.* International Journal of Hydrogen Energy, 2017. 42(11): p. 7275–7289.
19. *CoolProp*.
20. Leachman, J.W., et al., *Fundamental Equations of State for Parahydrogen, Normal Hydrogen, and Orthohydrogen.* Journal of Physical and Chemical Reference Data, 2009. 38(3): p. 721–748.
21. Fjeld, D., et al., *A common Nordic-Baltic costing framework for road, rail and sea transport of roundwood*. 2021, NIBIO.
22. Tayarani, H. and A. Ramji, *Life Cycle Assessment of Hydrogen Transportation Pathways via Pipelines and Truck Trailers: Implications as a Low Carbon Fuel.* Sustainability, 2022. 14(19).
23. Grønland, S.E., *Kostnadsmodeller for transport og logistikk. Basisår 2021*. 2022, Transportøkonomisk institutt - Stiftelsen Norsk senter for samferdsforskning.
24. Rexeis, M., M. Röck, and S. Hausberger, *Comparison of fuel consumption and emissions for representative heavy-duty vehicles in Europe*. 2018, International Council on Clean Transportation.
25. Elgowainy, A., et al., *Techno-economic and thermodynamic analysis of pre-cooling systems at gaseous hydrogen refueling stations.* International Journal of Hydrogen Energy, 2017. 42(49): p. 29067–29079.
26. Zhao, L., et al., *Review on studies of the emptying process of compressed hydrogen tanks.* International Journal of Hydrogen Energy, 2021. 46(43): p. 22554–22573.
27. Khan, M.A., et al., *The Techno-Economics of Hydrogen Compression*. 2021.
28. Skattetaten. *Vektårsavgift*. Available from: https://www.skatteetaten.no/satser/vektarsavgift/.

29. Songhurst, B., *The Outlook for Floating Storage and Regasification Units (FSRUs)*. 2017, Oxford Institute for Energy Studies.
30. SSB, *Lønn*. 2024.
31. Bundesnetzagentur, *Bundesnetzagentur publishes 2024 electricity market data*. 2025.
32. KG, N.P.G.C., *Port Tariff for the port managd by Niedersachsen Ports GmbH & Co. KG in Wilhemshaven*. 2025.
33. Mulligan, R.F., *A Simple Model for Estimating Newbuilding Costs.* Maritime Economics & Logistics, 2008.
34. Houchins, C., et al., *Final Summary Report for Hydrogen Storage System Cost Analyses (2017-2022)*. 2022, Strategic Analysis Inc.
35. Cepowski, T. and P. Chorab, *The Use of Artificial Neural Networks to Determine the Engine Power and Fuel Consumption of Modern Bulk Carriers, Tankers and Container Ships.* Energies, 2021. 14(16).
36. Rohner, C., *Daily Fuel Consumption and Greenhouse Gas Emissions by Bulk Carriers anchoring in the Southern Gulf Islands*. 2020, Salt Spring Island Climate Action Council.
37. Ship&Bunker. *Rotterdam Bunker Prices*. 2025; Available from: https://shipandbunker.com/prices/emea/nwe/nl-rtm-rotterdam.
38. Roussanaly, S., et al., *At what Pressure Shall CO2 Be Transported by Ship? An in-Depth Cost Comparison of 7 and 15 Barg Shipping.* Energies, 2021. 14(18).
39. SEND, P. *How Long Does it Take to Unload a Cargo Ship?* 2024 2025-10-28]; Available from: https://www.packsend.com.au/blog/unload-cargo-ship/.
40. *Bompengekalkulator*. Available from: https://bompengekalkulator.no.
41. *Secured Overnight Financing Rate Data*. Federal Reserve Bank of New York.
42. *Kostnadsindeks for vare- og lastebiltransport*. 2024, Statistisk Sentralbyrå.
43. Altinn. *Hva koster en arbeidstaker*. Available from: https://info.altinn.no/starte-og-drive/arbeidsforhold/ansettelse/hva-koster-en-arbeidstaker/.
44. Cox, J. *Fed slashes interest rates by a half point, an aggressive start to its first easing campaign in four years*. 2024; Available from: https://www.cnbc.com/2024/09/18/fed-cuts-rates-september-2024-.html.
45. Skattetaten. *Arbeidsgiveravgift*. 2024; Available from: https://www.skatteetaten.no/satser/arbeidsgiveravgift/.
46. Theis, J., *Quality Guidelines for Energy Systems Studies: Cost Estimation Methodology for NETL Assessments of Power Plant Performance*. 2021, National Energy Technology Laboratory (NETL), Pittsburgh, PA, Morgantown, WV, and Albany, OR (United States).
47. Worhach, P., *Recommended Project Finance Structures for the Economic Analysis of Fossil-Based Energy Projects*. 2011, National Energy Technology Laboratory.